First-principle molecular dynamics of the Berry pseudorotation: Insights on ^{19}F NMR in SF_4

Michele Pavone,[a] Vincenzo Barone,[a),c)] Ilaria Ciofini,[b)] and Carlo Adamo[b),d)]
Laboratorio di Struttura e Dinamica Molecolare, Dipartimento di Chimica, Complesso Universitario Monte Sant'Angelo, Via Cintia, I-80126 Napoli, Italy and Laboratoire d'Electrochimie et Chimie Analytique, UMR CNRS-ENSCP 7575 Ecole Nationale Supérieure de Chimie de Paris, 11 rue P. et M. Curie, F-75231 Paris Cedex 05, France

(Received 15 December 2003; accepted 25 February 2004)

First-principles [density-functional theory (DFT)] molecular-dynamic simulations of the Berry pseudorotation mechanism in SF_4 were performed using the atom-centered density-matrix propagation method. The reaction was monitored by following the chemical shieldings of the fluorine atoms, computed on snapshots along the trajectories. In particular we compared the results obtained using a standard functional based on the generalized gradient approximation with those issuing from its hybrid Hartree–Fock–DFT counterpart using a number of basis sets. Our results show that both the basis set and the functional choice rule the quality of the molecular properties monitored as well as the trajectory over the potential-energy surface. © *2004 American Institute of Physics.* [DOI: 10.1063/1.1707012]

I. INTRODUCTION

The so-called Berry pseudorotation reaction (BPR) (Refs. 1 and 2) has been evoked as the crucial step in many mechanisms of catalysis, even in those concerning biological systems. For instance, BPR is involved in the hydrolysis of phosphates, amides, and esters.[3] Also, some metal-phosphorane complexes of iron, cobalt, and ruthenium show a catalytic behavior that depends on the structural reorganization of the ligands through a pseudorotation dynamics.[4,5] Moreover, the properties and the dynamics of hypervalent compounds, typically undergoing a BPR, gained some relevance for their potential use as energetic materials.[6]

In the BPR mechanism a penta-coordinated system in a trigonal bipyramid (TBP) structure undergoes a simple exchange of the ligand coordination sites between the axial and the equatorial positions. During this process, none of the ligands leaves the coordination sphere of the central metal atom, and the transition state (TS) is characterized by a square-based pyramidal (SBP) geometry.

A very simple prototype molecule that undergoes a BPR is SF_4.[7] This molecule has C_{2v} symmetry, arising from a trigonal bipyramid arrangement with one vacant equatorial site.[8–10] Evidences of the BPR in SF_4 have been experimentally given by ^{19}F-NMR both in solution[11–13] and in the gas phase.[14] Actually SF_4 is one of the smallest molecules that undergoes an intramolecular rearrangement with rate constants accessible to NMR measurement.[13(a)] Nevertheless, also due to difficulties in the measurements (presence of impurities,[11(c),11(d)] bimolecular reactions[11(c),12]) it took many years to experimentally assess the energy barrier value for the topomerization reaction. Quite recently, NMR investigations established definitely activation barriers of 11.3 (Ref. 14) and 11.2 kcal/mol [Ref. 11(e)] for vapor and liquid SF_4, respectively.

At the same time, the BPR mechanism has been extensively investigated, using first-principle methods, for small hypervalent systems, such as SF_4 (Refs. 15–19) or PF_5.[20–21] These systems have been chosen as simple models to understand the behavior of larger and more complex systems, containing transition metals and fluxional phosphoranes or sulfuranes as ligands.[22] While a large number of such studies concerns the first-principle prediction of the thermochemistry of the BPR reaction,[15–20] some years ago Daul and co-workers[21] investigated the fluxional behavior of PF_5 using both a static approach (i.e., characterizing the extremants of the potential energy surface) and Car–Parrinello molecular dynamics.[23] These authors focused manly on the energetic analysis of the interconversion reaction and on the vibrational spectrum.[21]

Following this line, we present here a first-principle molecular-dynamics study of the magnetic properties of SF_4. When such a system undergoes a BPR, a simultaneous pairwise exchange of the axial fluorine atoms with the magnetically nonequivalent equatorial ones takes place. Therefore the BPR reaction can be followed calculating the change in ^{19}F nuclear magnetic shielding along the topomerization pathway, in strict resemblance with experiments. Furthermore, due to the fast exchange kinetics in SF_4, the study of BPR for this molecule is particularly appealing for a first-principle molecular-dynamic modeling since the pseudorotation takes place in a reasonable time scale (picoseconds). In order to obtain a full *ab initio* characterization of this intramolecular rearrangement, we have performed static and dynamic simulations, using methods rooted in the density-functional theory (DFT).[24] In this framework, the Car–Parrinello (CP) method[23] is well recognized as a powerful tool to investigate the dynamical behavior of chemical

[a)]Università di Napoli "Federico II."
[b)]ENSCP.
[c)]Corresponding author. Electronic mail: baronev@unina.it
[d)]Corresponding author. Electronic mail: adamo@ext.jussieu.fr

systems.[25] This method is based on an extended Lagrangian molecular-dynamics (MD) scheme, where the potential-energy surface is evaluated at the DFT level and both the electronic and nuclear degrees of freedom are propagated as dynamical variables.[23] The most recent implementations of the CP approach allow computing classical trajectories for quite large systems. Next, accurate spectroscopic (e.g., NMR) parameters can be obtained, as average values, using selected geometries along the trajectories.[26,27]

In the usual CP implementation, a plane-wave basis set is used, at variance with standard molecular quantum chemical approaches that employ localized (Gaussian or Slater) atomic basis, that allow for an easier and more direct interpretation in terms of classical chemical concepts. At the same time, the combined use of plane waves and pseudopotentials in the CP approach makes the use of hybrid Hartree–Fock/DFT functionals practically unaffordable.[28] Such functionals have been demonstrated to offer a significant improvement over conventional generalized gradient approximations (GGA), used in CP, especially for spectroscopic quantities.[29]

For these reasons, we use in this work the atom-centered density-matrix propagation (ADMP) method, a recent extension of the original CP approach in which the density matrix is propagated together with the nuclear degrees of freedom.[30–32] Thus Gaussian (or Slater) functions can be used to form an atom-centered basis set, providing a more flexible tool for the study of chemical systems and allowing the use of different levels of theory for electronic structure calculations. For instance, the ADMP method allows us to compare trajectories and properties obtained with functionals based on the generalized gradient approximation (GGA), which can be used in the standard CP-MD, with those computed with hybrid functionals. In particular, in the present paper we compare the performances of a GGA functional (BLYP) with those of its hybrid extension (B3LYP) for static calculations, generation of trajectories, and computation of average spectroscopic parameters. The ^{19}F nuclear magnetic shieldings (and the corresponding chemical shifts) have been calculated on a number of snapshots extracted from ADMP trajectories. This comparison will allow us to decouple the direct effect of the functional on the magnetic properties calculations from the indirect, structural one.

II. COMPUTATIONAL DETAILS

All the calculations have been carried out with the last version of the GAUSSIAN package.[33] Both gradient corrected Becke exchange[34] and Lee–Yang–Parr correlation[35] functionals (BLYP) and the corresponding Hartree–Fock–DFT hybrid functional [B3LYP (Ref. 36)] were used. In order to select the most effective basis set for the MD simulations, we tested different members of the Pople[37–40] and correlation consistent[41] series. For each basis set we have optimized the structure of the ground state (GS) and of the transition state (TS), computed the corresponding harmonic frequencies and zero-point energies (ZPE's), and evaluated ^{19}F-NMR shielding constants. On the basis of these results, ADMP simulations were carried out with both BLYP and B3LYP functionals, using the 6-31+G(d) basis set on the fluorine atoms and the 6-311G(3df) basis set for the sulfur atom. The simulations were performed at 298 and 550 K, for a total simulation time of 1.0 ps at 550 K and 2.0 ps at 298 K. For each simulation the starting point was the minimum structure obtained with the corresponding functional and the same basis set of MD runs. The Verlet algorithm,[43] for the integration of the equations of motions, and a time step of 0.25 fs were used, while the Cholesky decomposition[44] was chosen to obtain the unitary transformation of the density matrix into an orthonormal basis. The fictitious mass of the electron was set to 0.20 amu and it was scaled for core and valence electrons, as described in Ref. 32. The velocities of the nuclei were scaled each five time steps to ensure a constant temperature within a 5-K tolerance. The stability of the simulations was monitored by checking the idempotency of the density matrix (within a 10^{-12} threshold) and the so-called adiabaticity index (within a 10^{-4} threshold, see Ref. 31 for details).

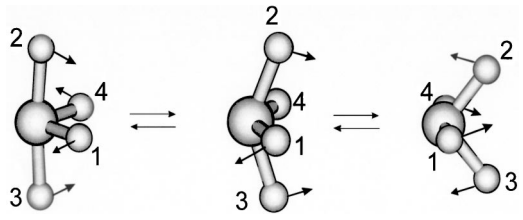

FIG. 1. Schematic sketch and labeling scheme for the minimum-energy structure and for the transition state of SF_4 BPR. The normal mode dominating the BPR is also indicated.

The ^{19}F NMR shieldings were computed using the gauge invatiant atomic orbital (GIAO) approach[42] and the 6-311++G(2d,2p) basis set on a number of snapshot extracted from the trajectories and on all the optimized structures (minima and saddle points). The basis set convergence with respect to the nuclear magnetic shielding calculations was checked on the SF_4 experimental structure[9] with different basis sets, ranging from 6-31G(d) to aug-cc-pVQZ.[37–41] In order to obtain chemical shifts consistent with experimental values,[13,14] the ^{19}F shielding of $CFCl_3$ was computed at the same level of theory on the optimized structure at the BLYP and the B3LYP levels.

Representative snapshots for NMR computations were taken each 5.0 fs in the time frame needed to complete the BPR mechanism at 550 K, for a total of 40 points for both the B3LYP and the BLYP trajectories. In the case of simulations at 298 K, the snapshots were extracted each 10 fs, for a total of 200 different structures, both for B3LYP and BLYP runs.

III. RESULTS AND DISCUSSION

A. Static calculations: Basis set assessment, structure, and activation energies

The structure and labeling of the molecule are reported in Fig. 1. As mentioned in the introduction, several theoretical studies concerning the prediction of BPR activation energy for the SF_4 molecule have already been reported in literature.[15–19] In these works the joint use of several density functionals and of medium size basis sets [6-31G(d), 6-311+G(d)], for the prediction of the activation enthalpy ($\Delta H^{\#}$)

TABLE I. Effect of the basis set tests on the properties of SF_4. Energies in kcal/mol, distances in Å, and chemical shieldings in ppm. Computed $\Delta\sigma(^{19}F_{ax}-^{19}F_{eq})$ in ppm.[a]

	Basis set (fluorine/sulphur)	$\Delta H^{\#}$	$\Delta G^{\#}$	$d(S\cdots F_{ax})$	$d(S\cdots F_{eq})$	$\Delta\sigma(^{19}F_{ax}-^{19}F_{eq})$
A	6-31G(d)	7.2	8.0	1.672	1.595	45.3
B	6-311+G(d)	8.3	9.1	1.704	1.597	56.2
C	6-31+G(d)/6-311G(2d)	9.4	10.2	1.680	1.579	58.7
D	6-31+G(d)/6-311G(3df) (MD03 basis)	10.3	11.1	1.673	1.572	59.9
E	6-311+G(3df)	10.0	10.8	1.670	1.566	60.7
F	cc-pVTZ	9.7	10.4	1.676	1.575	58.5
G	cc-pV(T+d)Z	10.2	11.0	1.664	1.565	60.1
H	cc-pV(Q+d)Z	10.1	10.9	1.666	1.564	60.9
I	aug-cc-p(Q+d)Z	10.1	10.9	1.668	1.563	61.6
	expt.[b]	11.3	12.2	1.646	1.545	60.9

[a]B3LYP/6-311++G(2d,2p) level of theory.
[b]Reference 14.

governing the BPR underestimate systematically $\Delta H^{\#}$ by about 3 kcal/mol with respect to the experimental value.[14,19] Although this shortcoming was ascribed to the limitations of current density functionals, recent studies on other molecules containing sulfur[41(c),45] suggest that medium size conventional basis sets are not sufficient for quantitative work. In order to check this point we have performed a systematic basis set study, whose main results are summarized in Table I and Fig. 2.

As a first point the activation enthalpy computed at the BLYP level is systematically lower by 1 kcal/mol than its B3LYP counterpart, which, in turn, reaches an asymptotic value about 1 kcal/mol lower than the experimental finding. Furthermore, only basis sets containing at least three *d* and one *f* function on sulfur provide converged structural parameters and activation barriers. Moreover, the computed activation entropy (about 0.8 kcal/mol) is in good agreement with experiment.

At this level the bond lengths are slightly overestimated with respect to the experimental data (by about 0.02 Å), but the difference between equatorial and axial SF bond lengths matches very well the experimental value. At the same time valence angles are always reproduced quite accurately. Next, computation of chemical shifts show that we can obtain a very good reproduction of the experimental data by single point B3LYP/6-311+G(2d) level at the experimental geometry or at all the optimized geometries showing a correct difference between axial and equatorial SF bond lengths.

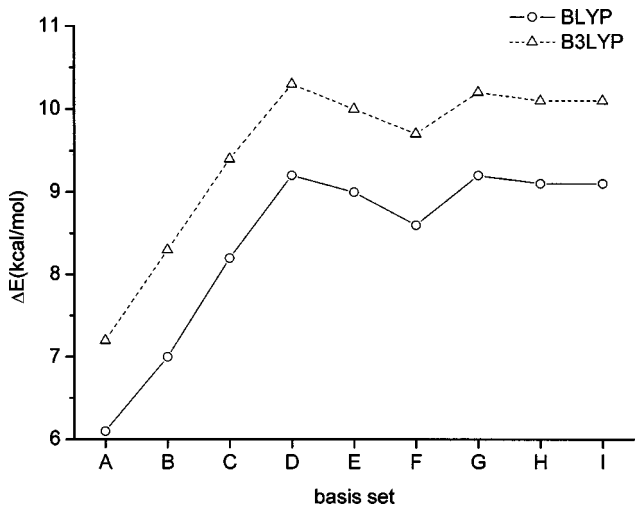

FIG. 2. Energy barriers computed by the different basis sets listed in Table VI.

In this context, once we have demonstrated the reliability of a DFT approach in the study of this molecule both for energies and for spectroscopic parameter prevision, we have selected for the ADMP simulations the combination of 6-31+G(d) and 6-311G(3df) basis sets on F and S atoms, respectively. This basis set (referred to in the following as MD03) offers, in our opinion, the best compromise between reliability and computational cost.

A comparison between the BLYP and the B3LYP results obtained with the MD03 basis set is reported in Table II.

The bond distances computed at B3LYP level are closer to the experimental values than their BLYP counterparts; the computed angles, instead, do not show significant differences between the two approaches. The computed energy barrier governing for the BPR processes ($\Delta E^{\#}=E_{TS}-E_{GS}$) and zero-point energy (ZPE) corrections are in reasonable agreement with the experimental values estimated from the analysis of exchange broadening in the gas phase ^{19}F NMR spectra.[14] As mentioned above, the energy barrier computed at the BLYP level is about 10% (~1 kcal/mol) lower than the B3LYP one since the introduction of some Hartree–Fock (HF) exchange reduces the overstabilization of symmetric delocalized structures characteristic of GGA functionals.[46] It

TABLE II. Thermochemical parameters (kcal/mol) and frequencies of the transition vectors (cm^{-1}) computed for SF_4 using the MD03 basis set.

	BLYP	B3LYP	Expt.[a]
$\Delta H^{\#}$	9.3	10.2	11.3(0.4)
$\Delta G^{\#}$	10.0	11.0	12.2(0.1)
ZPE_{GS}	6.4	7.3	
ZPE_{TS}	6.1	7.0	
ν_{TV}	137*i*	154*i*	

[a]Reference 14, in brackets experimental errors.

TABLE III. Harmonic frequencies (in cm^{-1}) and (in brackets) IR intensities (in km/mol) of SF_4 computed using different basis sets.

Assignment[a]	HF/ 6-31G(d)[b]	BLYP/ MD03	B3LYP/ MD03	B3LYP/ 6-311+G(3df)	B3LYP/ aug-cc-pV(Q+d)Z	Expt.[c]
A_1 (ν_4)	210(1)	201(0.9)	219(0.9)	215(0.9)	217(0.9)	223
B_2 (ν_9)	355(16)	297(8)	333(9)	335(9)	336(9)	353
A_2 (ν_5)	460(0)	394(0)	435(0)	439(0)	446(0)	414
A_1 (ν_3)	518(39)	448(13)	499(19)	501(18)	506(19)	475
B_1 (ν_7)	522(5)	454(2)	501(0.3)	504(0.6)	512(0.7)	532
A_1 (ν_2)	584(2)	496(5)	538(4)	533(3)	533(3)	558
B_2 (ν_8)	769(689)	675(590)	714(647)	705(629)	701(630)	730
B_1 (ν_6)	889(185)	750(171)	824(178)	824(173)	830(172)	867
A_1 (ν_1)	893(138)	787(101)	857(112)	858(107)	864(107)	892

[a]Assignment following Ref. 49.
[b]Scaled HF (scaling factor 0.893) values computed on MP2/6-31G(d) geometries taken from Ref. 18.
[c]Experimental values from Ref. 18.

is clear that this effect has also a relevant influence in the computed MD trajectories (*vide infra*).

The computed frequencies for the GS structure, in the harmonic approximation, are reported in Table III, together with their assignment and the available experimental data.[8(d)]

There has been a considerable discussion concerning the assignment of the ν_6 and ν_8 vibrations.[8(d),14,18,47–49] In particular previous experimental works suggest a B_2 symmetry for ν_6 and a B_1 symmetry for ν_8.[8d] In agreement with previous theoretical works,[18] we find the experimental assignment of Frey[49] more consistent with our results, so that ν_6 and ν_8 have B_1 and B_2 symmetry, respectively. The vibrational frequencies obtained with the B3LYP and BLYP functionals using the MD03, 6-311+G(3df), and aug-cc-pV(Q+d)Z basis sets are in fair agreement with the experimental data, although all the frequencies computed with the BLYP functional are systematically underestimated. Nevertheless, both the B3LYP and BLYP results (not scaled) are of the same accuracy as previous G2 and scaled DFT results.[14,18]

B. Molecular dynamics: Structure and thermochemistry

The ADMP simulations using the BLYP and B3LYP functionals were carried out starting from the optimized structure, since the same starting conditions for the two simulations allow for a more straightforward comparison between the two dynamics. The calculated total energy of the system (scaled with respect to the total energy of the starting point) as a function of time is reported in Fig. 3 for simulations at 298 and 550 K.

A survey of the plots clearly shows that the BPR takes place only in the simulations performed at the higher temperature (550 K). It is worth noting that a different initial kinetic energy was given for the two sets of simulations: 0.5 hartree/mol for the 298-K simulation and 1.0 hartree/mol for 550 K. The simulations at 298 K were used to extract the average structural and magnetic parameters reported in Tables IV and V, respectively.

From a structural point of view, we can notice that, as expected, the average distances computed on the ADMP trajectories are quite close (within 0.01 Å) to the optimized values, the molecule simply vibrating around its equilibrium structure. This behavior holds for both BLYP and B3LYP trajectories, even if the energy evolution shows, as expected, significant differences [see Fig. 3(a)]. The same problems (overestimation of bond lengths) and differences between

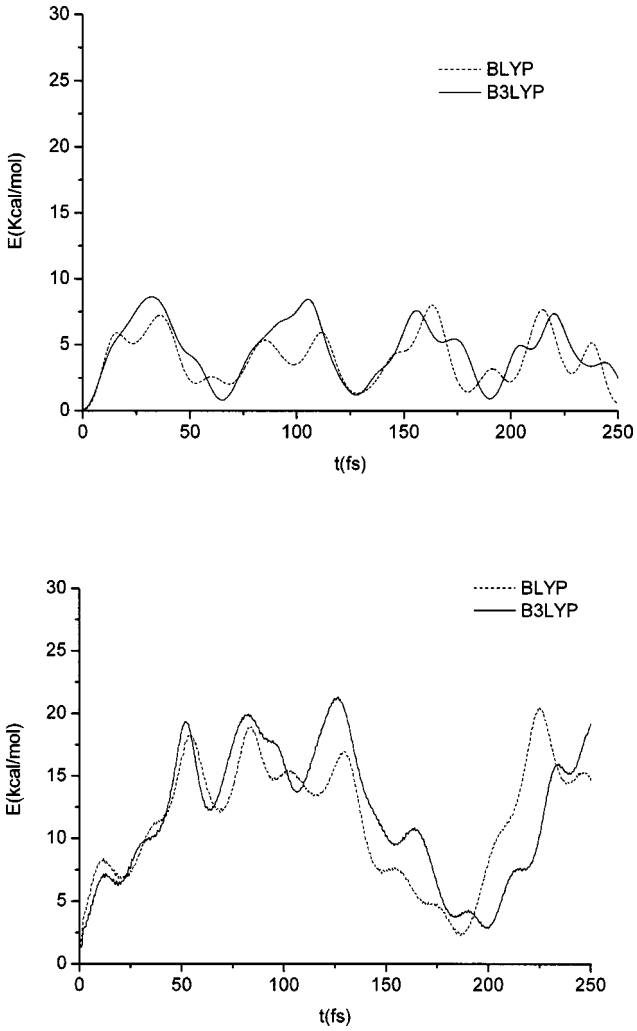

FIG. 3. Total energy of SF_4 calculated during the ADMP simulation at 298 K [(a), top] and 550 K [(b), bottom]. Full line: B3LYP; dotted line: BLYP.

TABLE IV. Optimized and average structures for the ground (GS) and transition state (TS) of SF_4 computed using the MD03 basis set. Distances in Å, angle in degrees.

	$GS(C_{2v})$				
	BLYP	$\langle BLYP\rangle_{298\ K}$	B3LYP	$\langle B3LYP\rangle_{298\ K}$	Expt.[a]
$d(S\text{-}F_{ax})$	1.708	1.732	1.672	1.678	1.646
$d(S\text{-}F_{eq})$	1.606	1.611	1.573	1.577	1.545
$a(F_{ax}SF_{ax})$	174.7		173.2		173.4
$a(F_{eq}SF_{eq})$	100.6		101.1		101.3
			$TS(C_{4v})$		
	BLYP		B3LYP		
$d(S\text{-}F_{ax})$	1.667		1.631		
$a(FSF)_{cis}$	83.7		83.5		
$a(FSF)_{trans}$	141.3		140.7		

[a]Reference 9.

BLYP and B3LYP results discussed in the static calculations still hold. On the other hand, the simulations at 550 K allow following the dynamics of the topomerisation. Both the BLYP and B3LYP functionals predict the BPR to take place, but some differences between the two calculated trajectories can be noticed. In particular, BLYP predicts a time scale for the whole reaction shorter than its B3LYP counterparts by about 25 fs. This is clearly shown by the calculated shielding constants along the trajectories (see below). Furthermore, this is consistent with the static calculations where a higher energy barrier is predicted at the B3LYP level with respect to the BLYP one.

In order to better rationalize the differences in the overall shape of the ADMP potential-energy profiles at 550 K, we can make reference to the frequencies computed both for the minimum-energy structures and for the transition states (Table III). The normal mode responsible for BPR (schematically depicted in Fig. 1) is the most important.

In the minimum-energy structure, this mode, of A_1 symmetry, has a harmonic frequency of 201 and 219 cm^{-1} at the BLYP and B3LYP level, respectively. The TS is, instead, characterized by a transition vector of B_1 symmetry with an imaginary frequency of $137i$ and $154i$ cm^{-1} for the two functionals. Although these values are computed in a simple harmonic approximation, they give a flavor of the curvature of the potential-energy surface (PES) along the normal coordinate responsible for the BPR. It is therefore noteworthy that the BLYP functional not only underestimates the energy barrier more severely than the B3LYP one, but also underestimates the curvature of the PES near the TS. Furthermore, from the simulation performed at 298 K, we can also notice that the molecule tends to stay near the starting energy minimum for a time longer at the BLYP than at the B3LYP level. This is again consistent with the flatter PES surface computed along the A_1 harmonic mode of the minimum-energy structure. The overall picture is therefore completely consistent with the results of the ADMP simulations reported in Fig. 3. More in general, we can conclude that the predictions concerning both the thermochemistry and the kinetics of the reaction significantly depend on the functional used to describe the PES for both static and dynamic simulations.

TABLE V. ^{19}F NMR chemical shifts (in ppm with respect to $CFCl_3$[a]) computed using the 6-311+G(2d) basis set on ADMP trajectories generated using the MD03 basis set.

	Static GS			298-K ADMP trajectory			
Geometry/ property[a]	BLYP/ BLYP	BLYP/ B3LYP	B3LYP/ B3LYP	BLYP/ BLYP	BLYP/ B3LYP	B3LYP/ B3LYP	Expt.[b]
δF_{ax}	118.7	122.7	106.6	135.0	133.1	114.8	93.74
δF_{eq}	64.7	65.2	46.7	83.7	76.9	55.8	32.84
$\delta F_{ax}-\delta F_{eq}$	54.0	57.5	59.9	51.9	56.2	59.0	60.90

[a]Absolute shielding of reference BLYP/BLYP: 113.9 ppm; BLYP/B3LYP: 142.0 ppm; B3LYP/B3LYP: 155.5 ppm.
[b]References 13 and 14.

C. NMR calculations

As mentioned before, the NMR spectrum of SF_4 has been well characterized: a ^{19}F chemical shift of 93.74 ppm for the axial fluorines and of 32.84 ppm for the equatorial ones were measured in the gas phase at 213 K, taking as reference $CFCl_3$.[13,14]

Early coupled-HF calculations yielded a chemical shift difference between axial and equatorial fluorines of 64.1 and 86.5 ppm depending on gauge choice to be compared with an

TABLE VI. Computed absolute nuclear magnetic shielding (in ppm) as a function of the basis set. B3LYP calculations on experimental structure.[a]

Basis set	No. basis functions	$^{19}F_{ax}$	$^{19}F_{eq}$	$^{19}F_{ax}-{}^{19}F_{eq}$
6-31G(d)	79	89.9	159.7	69.8
6-31+G(d)	99	96.7	153.1	56.4
MD03	115	93.4	154.4	61.0
6-311+G(d)	118	76.2	137.5	61.3
6-311+G(2d)	143	69.9	134.0	64.1
6-311+G(3df)	203	70.1	136.1	66.0
IGLO II	123	81.8	141.6	60.0
IGLO III	184	67.3	130.9	63.6
aug-cc-pVDZ	119	101.4	155.3	53.9
aug-cc-pVTZ	234	80.5	141.2	60.7
aug-cc-pVQZ	404	71.2	135.5	64.3
Expt.[a]				60.9

[a]Reference 9.
[b]Reference 13.

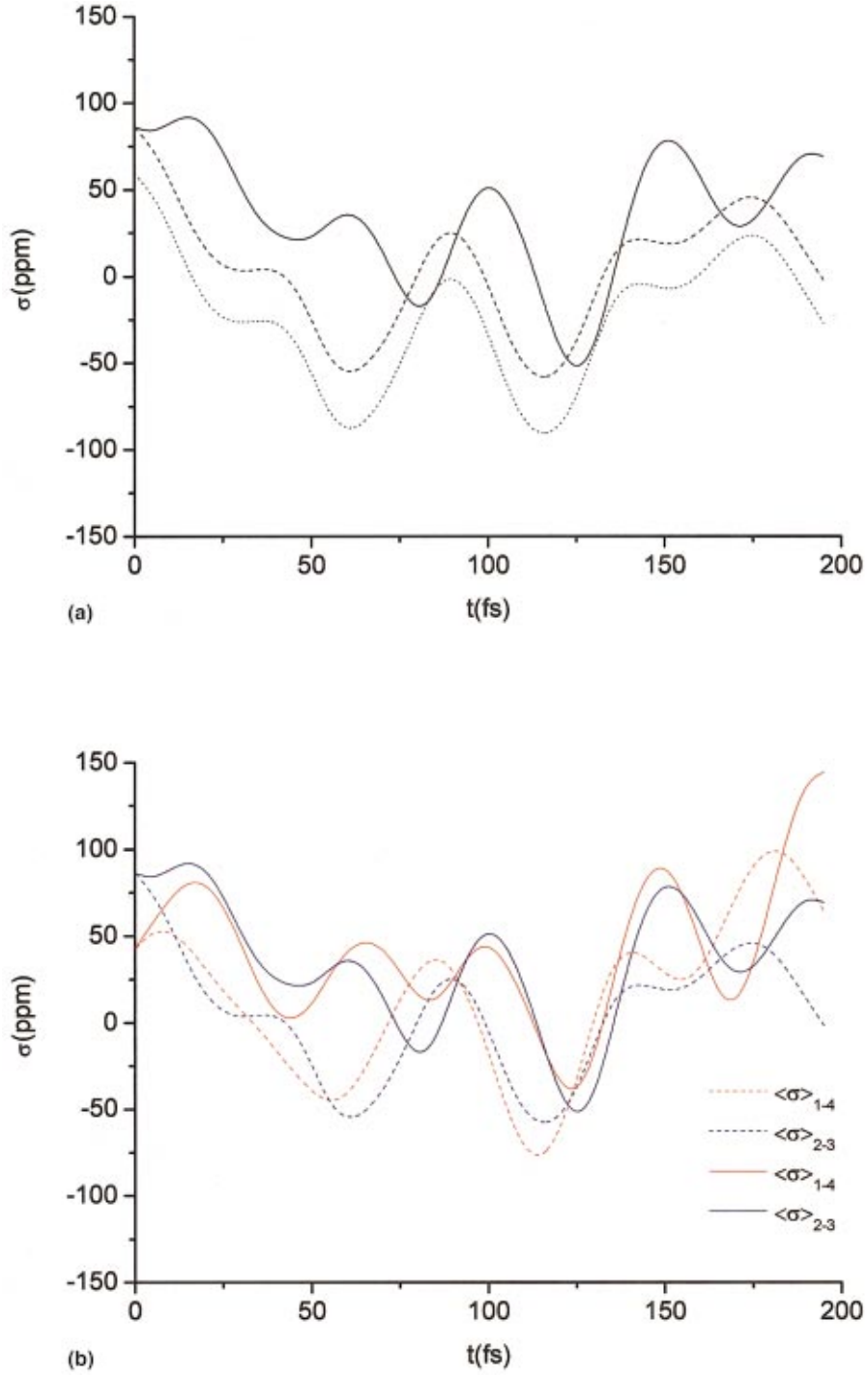

FIG. 4. (Color) (a) Computed ^{19}F absolute shielding along the ADMP trajectories. Average of $\sigma(F_1)$ and $\sigma(F_4)$ are reported. Full line: ADMP-B3LYP/GIAO-B3LYP; dashed line: ADMP-BLYP/GIAO-B3LYP; dotted line: ADMP-BLYP/GIAO-BLYP. (b) Computed ^{19}F absolute shielding along the ADMP trajectories. Full line: ADMP-B3LYP/GIAO-B3LYP; dotted line: ADMP-BLYP/GIAO-B3LYP. Red line: average of $\sigma(F_1)$ and $\sigma(F_4)$ ($\langle\sigma_{1-4}\rangle$); blue line: average of $\sigma(F_2)$ and $\sigma(F_3)$ ($\langle\sigma_{2-3}\rangle$).

experimental value of 60.9 ppm.[49] To the best of our knowledge, these are the only NMR calculations on SF_4 published insofar.

The first step of our study was the assessment of the most effective basis set for NMR calculations. This point is of particular relevance, since we have to perform a series of calculations of shielding tensor on a relatively large number of snapshots extracted from MD simulations, and therefore we seek for a reasonable compromise between basis set quality and computational burden. In Table VI are reported the fluorine absolute chemical shifts computed at the experimental geometry with several basis sets, ranging from a polarized valence double-ζ [6-31G(d)] to a large quintuple-ζ basis set, including diffuse and polarized functions (aug-cc-pVQZ).

From the results reported in this table, it clearly appears that the 6-311+G(2d) basis set, a medium-size basis, performs a very good job, since it gives results comparable to those issuing from the largest basis sets with significantly shorter computer times. This basis set has been already used for NMR studies (see, for instance, Ref. 50). At the same time, the computed differences between the axial and equatorial shieldings are very close to the experimental value (last line of Table VI). Moreover, calculations carried out with the 6-311+G(2d) basis set and the GS geometry obtained with a

large basis set, for example, cc-pV(Q+d)Z, give $\sigma(^{19}F_{ax}) - \sigma(^{19}F_{eq})$ of 60.9 ppm, in close agreement with the experimental value (60.9 ppm) and the value computed on the experimental geometry (64.1 ppm) at the same level of theory. It must be also pointed out that the MD03 basis set provides absolute chemical shifts which are significantly overestimated, while the difference is close to the experimental value.

The computed chemical shifts obtained both from calculations on the optimized structure and as average values computed on snapshots taken from the 298-K MD are reported in Table V, together with the experimental data.[13] Let us first analyze the results on optimized structures, in order to rationalize the effects of the functional on the property. By comparing the results obtained using the BLYP geometry with those obtained using the B3LYP one we can draw two main conclusions. First there is a better agreement of the B3LYP data with experiments. This is due both to geometrical (change in structure between the optimized BLYP and B3LYP values) and to direct (change of functional for NMR prediction at constant geometry) effects. Second, and more interestingly, these two effects are of the same order of magnitude and they affect the prediction both of chemical shifts of axial and equatorial fluorines, as well as their difference. Therefore in order to get reliable descriptions of NMR parameters of a molecular system, both geometrical and direct effects have to be taken into account, or, differently said, both the PES and the properties should be computed at a reliable level of theory.

The results obtained using the snapshots extracted from the dynamics at 298 K follow the behavior found for the static calculations, even if a slightly smaller difference in the fluorine chemical shifts is found. This difference is larger for the calculations carried out at BLYP geometries, due to the flatter PES, as discussed above.

More interesting are the results of ADMP simulations at 550 K. We recall that all the fluorine atoms are equivalent by symmetry at the TS, whereas the axial and equatorial fluorine atoms have different nuclear magnetic shieldings at the minimum-energy structure. In Fig. 4(a), the shieldings computed for a number of snapshots along the BLYP and B3LYP trajectories are reported. For the sake of clarity, only average values of the equivalent fluorine atoms (F_1 and F_4, see Fig. 1) are reported.

It is fairly clear from these plots that both direct and indirect effects are at work. In fact, when using the B3LYP functional for property evaluations at the geometries extracted from the BLYP trajectories a simple shift of the computed shielding is found with respect to the NMR values computed at BLYP level on the same trajectories. This is nicely illustrated by the two parallel plots in Figs. 4(a) and 4(b). A more drastic behavior is found, instead, when the B3LYP functional is used for property and trajectory evaluations. In this case, in fact, not only larger values of the shielding but a complete different dynamic effect are found. This result is even more evident when directly comparing the shielding computed at B3LYP level on BLYP snapshots or on B3LYP snapshots as done in Fig. 4(b). In particular, we can see that at the ADMP-BLYP level of theory, the BPR reaches the TS only after 15 fs (one equivalent signal for all F atoms) while a longer period is needed when using the ADMP-B3LYP approach (roughly 30 fs). Furthermore, at the BLYP level after 180 fs the BPR mechanism is complete and the two pairs of fluorine atoms already inverted, while a period of almost 200 fs is necessary at the B3LYP level. At the same time, the computed absolute shielding values are also significantly different, as already found in the static calculations. In conclusion, our results show that the prediction of NMR properties using a MD approach depend not only on the level of theory used for property evaluations, but also on the indirect effect of structure on the molecular property of interest, i.e., on the level of theory used for the scan of the PES.

IV. CONCLUSIONS

From the analysis of the simple intramolecular interconversion dynamics of SF_4 in the gas phase, we highlighted the role that the level of theory (e.g., density-functional model and basis set) used in molecular-dynamics simulation has in property evaluations. In particular, using the ADMP approach, we directly compared results obtained from trajectories computed with a hybrid functional (here B3LYP) with their counterparts obtained using the parent GGA functional (here BLYP). Our results show that in full agreement with static calculations both direct (level of property calculations) and indirect (structural) effects are important for a correct estimate of NMR parameters. Therefore the choice of the functional becomes crucial also for molecular-dynamics calculations, as it is in static approaches. In this context, hybrid functionals can play a major role, as well as dynamic approaches using local atom-centered basis set.

ACKNOWLEDGMENTS

I.C. and C.A. thank CNRS for financial support from the ACI ''Jeune Equipe 2002'' project. M.P. is grateful to the ''Programma internazionale di mobilità docenti e studenti'' of the University of Naples for a grant. V.B. and M.P. thank the Italian University and Research Ministry (MIUR) for financial support and Dr. Nadia Rega (Naples University) for useful discussions.

[1] R. S. Berry, J. Chem. Phys. **32**, 933 (1960).
[2] R. S. Berry, Rev. Mod. Phys. **32**, 444 (1960).
[3] J. K. Bashkin, Curr. Opin. Chem. Biol. **3**, 752 (1999).
[4] H. Nakazawa, K. Kawamura, K. Kubo, and K. Miyoshi, Organometallics **18**, 2961 (1999).
[5] H. Nakazawa, K. Kawamura, T. Ogawa, and K. Miyoshi, Organometallics **646**, 204 (2002).
[6] J. Moc, Theochem J. Mol. Struct. **461**, 249 (1999).
[7] O. Ruff and A. Heinzelmann, Z. Anorg. Chem. **72**, 63 (1911).
[8] (a) R. E. Dodd, L. A. Woodward, and H. L. Roberts, Trans. Faraday Soc. **52**, 1052 (1956); (b) V. C. Ewing and L. E. Sutton, *ibid.* **59**, 1241 (1963); (c) I. W. Levin and C. V. Berney, J. Chem. Phys. **44**, 2557 (1966); (d) K. O. Christie and W. Sawodny, *ibid.* **52**, 6320 (1970).
[9] W. M. Tolles and W. D. Gwinn, J. Chem. Phys. **36**, 1119 (1962).
[10] K. Kimura and S. H. Bauer, J. Chem. Phys. **39**, 3172 (1963).
[11] (a) A. J. Pople, W. G. Schneider, and H. J. Bernstein, *High-Resolution Nuclear Magnetic Résonance* (McGraw-Hill, New York, 1959), p. 223; (b) L. E. Muetterties and W. D. Phillips, J. Am. Chem. Soc. **79**, 322 (1957); (c) **81**, 1084 (1959); (d) J. Chem. Phys. **46**, 2862 (1967); (e) F. Seel and W. J. Gombler, J. Fluorine Chem. **4**, 327 (1974).

[12] F. A. Cotton, J. W. George, and J. S. Waugh, J. Chem. Phys. **28**, 944 (1958).
[13] (a) W. G. Kempler, J. K. Krieger, M. D. McCreary, E. L. Muetterties, D. D. Traficante, and G. M. Whitesides, J. Am. Chem. Soc. **97**, 7023 (1975); (b) C. A. Spring and N. S. True, *ibid.* **105**, 7231 (1983).
[14] A. N. Taha, N. S. True, C. B. LeMaster, C. L. LeMaster, and S. M. Neugebauer-Crawford, J. Phys. Chem. A **104**, 3341 (2000).
[15] R. M. Minyaev and J. A. Yudelevich, J. Mol. Struct.: THEOCHEM **262**, 73 (1992).
[16] T. Ziegler and G. L. Gutsev, J. Chem. Phys. **96**, 7623 (1992).
[17] (a) K. O. Christe, D. A. Dixon, P. A. Mercier, J. C. P. Sanders, G. J. Schrobilgen, and W. W. Wilson, J. Am. Chem. Soc. **116**, 2850 (1994); (b) K. O. Christe, D. A. Dixon, G. J. Schrobilgen, and W. W. Wilson, *ibid.* **119**, 3918 (1997).
[18] K. K. Irikura, J. Chem. Phys. **102**, 5357 (1995).
[19] M. Mauksch and P. Von Raugé Shleyer, Inorg. Chem. **40**, 1756 (2001).
[20] H. Wasada and K. Hirao, J. Am. Chem. Soc. **114**, 16 (1992), and references therein.
[21] C. Daul, M. Frioud, O. Schafer, and A. Selloni, Chem. Phys. Lett. **262**, 74 (1996).
[22] (a) H. H. Michels and J. A. Montgomery, Jr., J. Chem. Phys. **93**, 1805 (1990); (b) A. Caligiana, V. Aquilanti, R. Burcl, N. C. Handy, and D. P. Tew, Chem. Phys. Lett. **369**, 335 (2003).
[23] R. Car and M. Parrinello, Phys. Rev. Lett. **55**, 2471 (1985).
[24] W. Kohn and L. J. Sham, Phys. Rev. **140**, A1133 (1965).
[25] G. Galli and A. Pasquarello, in *Computer Simulation in Chemical Physics*, edited by M. P. Allen and D. J. Tildesley (Kluwer, Dordrecht, 1994), p. 261.
[26] (a) V. G. Malkin, O. L. Malkina, G. Seinebrunner, and H. Huber, Chem.-Eur. J. **2**, 452 (1996); (b) B. G. Pfrommer, F. Mauri, and S. G. Louie, J. Am. Chem. Soc. **122**, 123 (2000); (c) D. Sebastiani and M. Parrinello, J. Phys. Chem. A **105**, 1951 (2001).
[27] (a) M. Bühl and M. Parrinello, Chem.-Eur. J. **7**, 4487 (2001); (b) M. Bühl, F. T. Mauschick, F. Terstegen, and B. Wrackmeyer, Angew. Chem., Int. Ed. Engl. **41**, 2312 (2002); (c) M. Bühl and F. T. Mauschick, Phys. Chem. Chem. Phys. **4**, 5508 (2002).
[28] D. A. Gibson, I. V. Ionova, and E. A. Carter, Chem. Phys. Lett. **240**, 261 (1995).
[29] See, for instance, C. Adamo, A. di Matteo, and V. Barone, Adv. Quantum Chem. **36**, 45 (1999).
[30] S. S. Iyengar, H. B. Shlegel, J. M. Millam, G. A. Voth, G. E. Scuseria, and M. J. Frish, J. Chem. Phys. **115**, 10291 (2001).
[31] H. B. Shlegel, J. M. Millam, S. S. Iyengar, G. A. Voth, A. D. Daniels, G. E. Scuseria, and M. J. Frish, J. Chem. Phys. **114**, 9758 (2001).
[32] H. B. Shlegel, S. S. Iyengar, X. Li, J. M. Millam, G. A. Voth, G. E. Scuseria, and M. J. Frish, J. Chem. Phys. **117**, 8694 (2002).
[33] M. J. Frisch, G. W. Trucks, H. B. Schlegel *et al.*, GAUSSIAN 03, Revision B.04, Gaussian, Inc., Pittsburgh, PA, 2003.
[34] A. D. Becke, Phys. Rev. A **38**, 3098 (1988).
[35] C. Lee, W. Yang, and R. G. Parr, Phys. Rev. B **37**, 785 (1988).
[36] A. Becke, J. Chem. Phys. **98**, 5648 (1993).
[37] (a) P. C. Hariharan and J. A. Pople, Theor. Chim. Acta **28**, 213 (1973); (b) M. M. Francl, W. J. Petro, W. J. Hehre, J. S. Binkley, M. S. Gordon, D. J. DeFrees, and J. A. Pople, J. Chem. Phys. **77**, 3654 (1982).
[38] J. A. Pople, J. Chem. Phys. **72**, 650 (1980).
[39] J. P. Blaudeau, M. P. McGrath, L. A. Curtiss, and L. Radom, J. Chem. Phys. **107**, 5016 (1997).
[40] Diffuse exponents for F from: T. Clark, J. Chandrasekhar, and P. v. R. Schleyer, J. Comput. Chem. **4**, 294 (1983).
[41] (a) T. H. Dunning, Jr., J. Chem. Phys. **90**, 1007 (1989); (b) R. A. Kendall, T. H. Dunning, and R. J. Harrison, *ibid.* **96**, 6796 (1992); (c) T. H. Dunning, K. A. Peterson, and A. K. Wilson, *ibid.* **114**, 9244 (2001).
[42] W. Kutzelnigg, U. Fleischer, and M. Schindler, in *NMR Basic Principles and Progress*, edited by P. Diehl, E. Flick, H. Günter, R. Kosfeld, and J. Seelig (Springer-Verlag, Heidelberg, 1990), Vol. 23, pp. 165–262.
[43] W. C. Swope, H. C. Andersen, P. H. Berens, and K. R. Wilson, J. Chem. Phys. **76**, 637 (1982).
[44] G. H. Golub and C. F. Van Loan, *Matrix Computations* (The John Hopkins University Press, Baltimore, 1996).
[45] J. M. L. Martin, J. Chem. Phys. **108**, 2791 (1998).
[46] (a) H. Chermette, I. Ciofini, F. Mariotti, and C. Daul, J. Chem. Phys. **115**, 11068 (2001); (b) M. N. Glukhovtsev, R. D. Bach, A. Pross, and L. Radom, Chem. Phys. Lett. **260**, 558 (1996).
[47] I. W. Levin, J. Chem. Phys. **55**, 5393 (1971).
[48] P. Hassanzadeh and L. Andrews, J. Phys. Chem. **96**, 9177 (1992).
[49] R. A. Frey, R. L. Redington, and A. L. K. Aljibury, J. Chem. Phys. **34**, 344 (1971).
[50] J. R. Cheeseman, G. W. Trucks, T. A. Keith, and M. J. Frisch, J. Chem. Phys. **104**, 5497 (1998).